

Parallel Three-Dimensional Finite Element Bearing Capacity Analysis of c - ϕ soils

Mark D. Evans

United States Military Academy, West Point, NY, USA

D. V. Griffiths

Colorado School of Mines, Golden, CO, USA

Keywords: Numerical and analytical methods, bearing capacity, friction, cohesion, finite element, parallel, iterative solutions

ABSTRACT: Numerical analysis of large, complex structures in geotechnical engineering, especially in 3-d, is rarely performed because conventional finite element software leads to large global matrices that exceed the core memory of the computer. The resurgence of interest in iterative, highly parallelizable, solvers for large systems of linear equations now means that assembly of these large global matrices can be entirely avoided. This project will exploit recent developments in finite element software and the availability of high-speed parallel computer architecture to model large 3-d geotechnical problems previously considered beyond the reach of conventional analysis. This paper focuses on practical geotechnical analyses involving elasto-plastic material properties in bearing capacity analysis of c - ϕ soils by considering square and rectangular footings.

1 Introduction

Three-dimensional finite element analyses of bearing capacity are useful tools for practical problem solving as well as for parametric analysis and failure mechanism visualization. In this paper, the results of Mohr-Coulomb, elasto-viscoplastic, bearing capacity analyses were performed using finite element code running on massively parallel computers. Square, rectangular, and strip footings are considered in these analyses to determine bearing capacity factors and compare the determined values to those in the literature. With the recent advent of PC Clusters, parallel computing is readily available to those who may not have access to parallel supercomputers. Speedup values for increased numbers of processors in the parallel environment are also presented and discussed.

2 Bearing Capacity Of Shallow Footings

When a uniform pressure is applied over a finite area of the soil, the surface settles. Settlement curves are commonly used to relate pressure and settlement. For stiff soils, the bearing capacity is usually well-defined. However, for loose or soft soils, the bearing capacity is not so well defined and is typically described as the point on the curve where the settlement-pressure curve becomes steep and straight (Terzaghi and Peck, 1967).

For frictionless, cohesive soils, where $\phi = 0$ and $c > 0$, Prandtl (1921) determined that the bearing capacity per unit area is:

$$q_{ult} = cN_c = (2 + \pi)c = 5.14c \quad (1)$$

In this paper we shall consider weightless, cohesive and cohesionless soils possessing various friction angles. The effect of surface surcharge will also be considered. Thus, bearing capacity term γBN_f will be equal to zero, but the other bearing capacity factors, N_c , and N_q , will be explored. Prandtl defined N_c for frictional soils as:

$$N_c = (e^{\pi \tan \phi} \tan^2(45 + \phi / 2) - 1) \cot \quad (2)$$

When the ground surface is acted upon by a uniformly applied surcharge, q , the bearing capacity is increased by an amount qN_q , (Terzaghi and Peck, 1967) where:

$$N_q = e^{\pi \tan \phi} \tan^2(45 + \phi / 2) \quad (3)$$

Thus, N_c may be written as:

$$N_c = (N_q - 1) \cot \quad (4)$$

and finally:

$$\text{Bearing Capacity} = cN_c + qN_q \quad (5)$$

for weightless soils possessing cohesion, friction, or both.

Skempton (1951) proposed that the cN_c term be multiplied by a so-called "shape" factor to account for changes in bearing capacity for footings not of infinite length. He proposed the following shape factor:

$$s_c = (1 + 0.2B/L) \quad (6)$$

where B is the footing width and L is the footing length. A similar shape factor determined for the qN_q term is:

$$s_q = (1 + \tan \phi B/L) \quad (7)$$

Equation 5 then becomes:

$$\text{Bearing Capacity} = cN_c s_c + qN_q s_q \quad (8)$$

3 Finite Element Analyses

The paper presents the results of three-dimensional elasto-viscoplastic analyses of bearing capacity problems with a Mohr-Coulomb failure criterion. Plasticity is modelled via the elasto-viscoplastic algorithm (Zienkiewicz and Corneau, 1974) and the algorithm employs 20-node hexahedral elements with 8 integrating points (2x2x2) per element. This level of "reduced integration" has been shown to work effectively in both the stiffness and stress redistribution phases of the algorithm.

The program used in these studies is essentially the same as Program 12.2 in the text by Smith and Griffiths (2004) with minor modifications to allow different sizes of footing. All the source code from Smith and Griffiths (over 60 main programs for solving a wide range of engineering analysis) is written in Fortran 95 and is available on-line at the web site: www.mines.edu/fs_home/vgriffit/4th_ed. All the programs in Chapter 12 are written for execution using parallel processing computers such as those described in the next Section. Three-dimensional analyses such as those demonstrated in this paper are greatly facilitated by the use of iterative equation solvers that avoid the need to assemble and store large matrices such as the global stiffness matrix. In these studies, the Preconditioned Conjugate Gradient (pcg) method has been used (Smith and Griffiths, 2004) with diagonal preconditioning. The pcg method enables sophisticated 3-d analyses to be performed in a routine manner on either clusters of inexpensive desktop computers or massively parallel supercomputers like that used in this study.

4 Parallel Processing Computers

The analyses described in this paper were performed primarily on a US Department of Defense (DOD) supercomputer operated by the High Performance Computing Modernization Program (HPCMP) at the Army Research Laboratory (ARL) at Aberdeen Proving Ground, MD. The name of the particular machine used is Zornig. Zornig is an SGI Origin 3800, operating on the IRIX 6.5 operating system. On the unclassified side of Zornig, there are 512, R12000 processors operating at a processing speed of 400 MHz. The SGI 3800 is a shared memory multi-processor system, and Zornig has 384 Gbytes of shared memory (RAM) and employs MPI – Message Passing Interface – to pass information between processors. Zornig has a hard disk capacity of 5 Tbytes backed up by RAID storage.

Some analyses were also performed on a 16-node pc cluster located at USMA in the Dept of Civil and Mechanical Engineering. The cluster, named Chalk, consists of 16 Pentium 4 Processors operating at 2.0GHz with 512 MB of memory on each node. Timing and speedup results from both systems will be shown.

Parallel processing allows the main processor to slice up the work to be performed and scatter those computations to the various compute nodes (processors) allocated to the work. Each compute node is responsible for completing the assigned computations, after which the main processor will gather up all the data and reassemble it for output or for further computations. MPI (message passing interface) actually uses commands called "gather" and "scatter" as part of its routines.

Parallel processing allows very large jobs to be run in much shorter time. For example, one of the data sets described in this paper entailed loading a 2 x 2 square footing acting over the corner of a 10 x 10 x 16, 3D grid (with 2 axes of symmetry). This was one of the smaller grids used in this study, consisting of 800 elements with 4037 nodes and 10,064 equations of equilibrium. Soil properties were: $\phi=20^\circ$, $c=100$ units, poisons ratio = 0.30, and surcharge, $q = 0$; 10 pressure increments were applied to develop the pressure-settlement curve. When a single processor is used to solve this problem

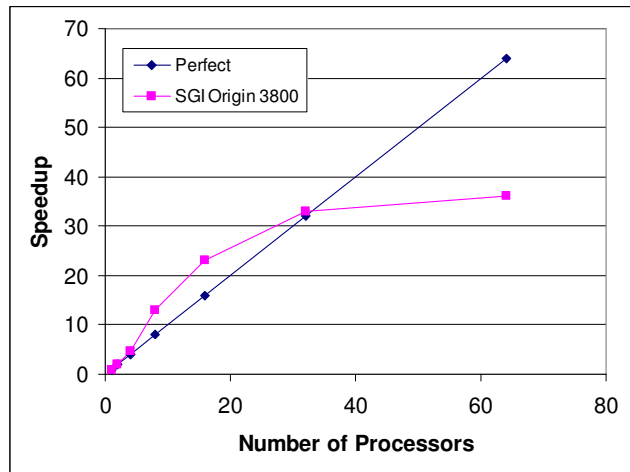
it would take 312 minutes (5.2 hours) to complete. However, by parallelizing the program, it took only 9.5 minutes to run on 32 processors. Table 1 shows the number of processors used versus the time to complete the analyses for this footing.

These data are plotted in Figure 1a where a 45° line is shown for comparison. The 45° line indicates “perfect speedup” – where there is no time lost sending packets of information between the multiple processors. However, in reality, there is inefficiency, or latency, in parallel computations where compute nodes may not be kept busy 100% of the time as data packets are passes between processors. In spite of this latency, the value of parallel processor computations should be evident in that the overall compute time decreases dramatically for greater numbers of processors. For the program used in these analyses, it may be seen that there is superlinear performance (compared to one processor) using 4 to 32 processors, after which speedup degrades, indicating that there is little value in using more than 32 processors for this particular program and data. Sixteen processors were used for most of the analyses presented in this paper, as a good balance between efficiency and processor availability.

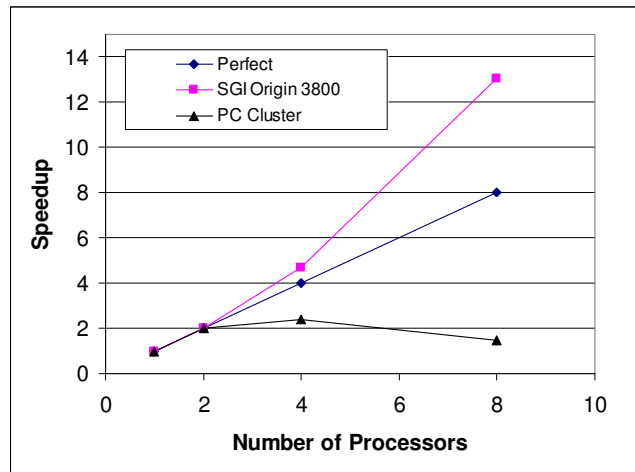
Figure 1b shows speedup data for the SGI Origin and the pc cluster. It may be seen in this figure that the SGI Origin performed much better than the cluster for all processor numbers greater than two. It may also be seen that the pc cluster speedup peaks at 4 processors, after which performance degrades. No attempt was made to optimize the code used to improve performance on these platforms. Code optimization for these platforms and others (Cray X1, others) will be investigated in future studies.

Table 1: Number of Processors vs. Compute Time (min)

Number of Processors	SGI Origin Compute Time (min)	PC Cluster Compute Time (min)
1	312 (estimated)	202 (estimated)
2	156	101
4	67	84
8	24	137
16	13.5	--
32	9.5	--
64	8.7	--



(a)

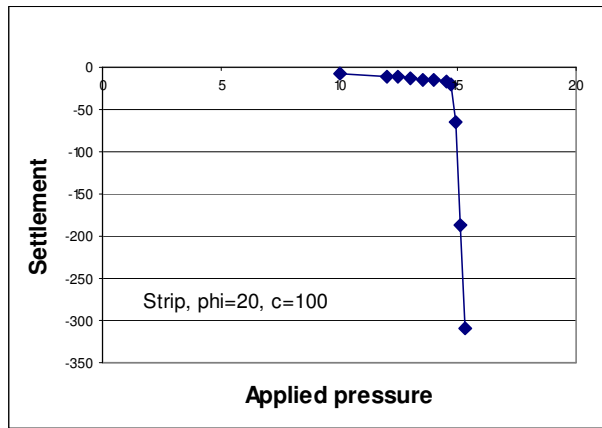


(b)

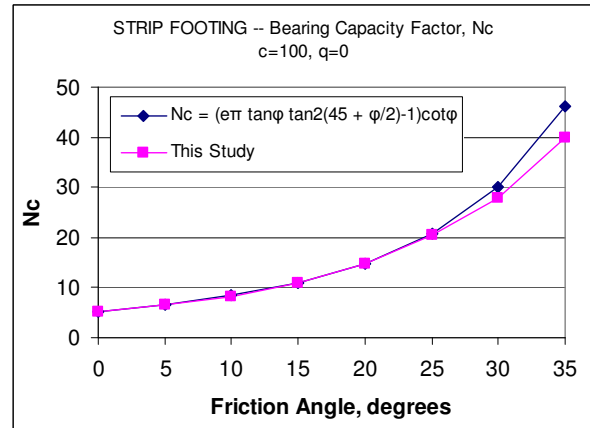
Figure 1. 800 Element Grid Speedup

5 Strip Footings

Footing pressure was applied incrementally and settlement determined for each increment, as shown in Figure 2a for a strip footing with $\phi=20^\circ$ and $c=100$. The numerical values of settlement shown in the figure are not particularly meaningful, rather they show small, gradual increases in settlement as pressure is increased followed by a rapid, steep increase in settlement after a particular value of pressure is applied. The point where the settlement curve increases steeply and becomes straight is defined by Terzaghi and Peck (1967) as the bearing capacity, and in Figure 2a, that value is approximately 14.7. Pressure values were normalized to cohesion so that the bearing capacity factor, N_q , could be plotted directly versus settlement, for a range of friction angles, as shown in Figure 2b. Since the values determined in this study are almost exactly the anticipated Prandtl theoretical values, especially for friction angles below 30° , the authors judged that the model was sufficiently accurate to warrant deeper investigation.



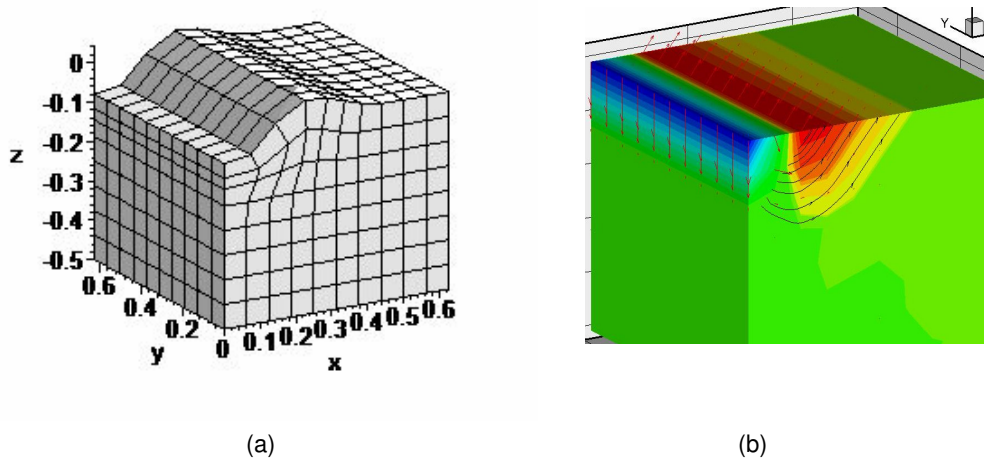
(a)



(b)

Figure 2. Typical Settlement vs. Pressure Curve and N_c vs Friction Angle for Strip Footings

Shown in Figure 3 are (a) the deformed mesh and (b) 3D displacement vectors, respectively, for a typical strip footing at bearing failure. It may be seen that both figures indicate a failure mechanism and zones of plastic equilibrium consistent with those described by Prandtl (1921) and Terzaghi and Peck (1967). Note the settlement under the loaded area and the surface heave outside the loaded footing area. The loaded areas of all strips were 20% of the mesh in plan view. Note how the failure mechanism zone extends out to about 60% of the mesh area in the plan view.



(a)

(b)

Figure 3. Deformed mesh and 3D Displacement vectors for Strip Footing

Additional analyses were performed on strip footings to determine how well N_q could be predicted. Cohesion was set to zero and surcharge pressure, q , set to a nominal value of 100 units of pressure. Then, bearing capacity was determined for a range of friction angles. Values determined in this study are shown in Figure 4 along with values determined by equation 3. It may be seen that there is good agreement between theoretical and finite element-determined values.

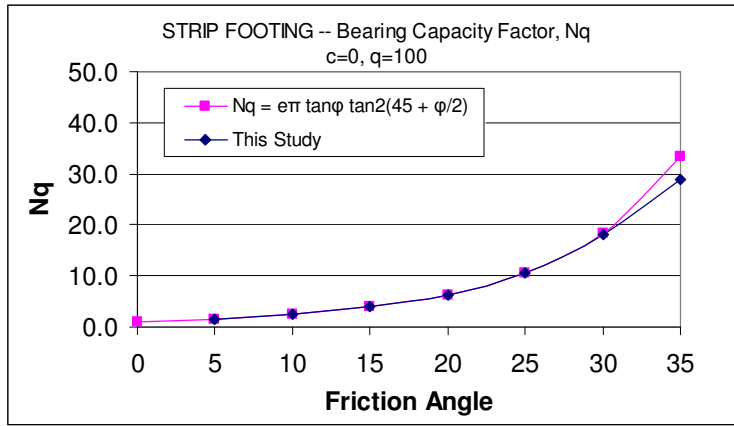


Figure 4. N_q vs. Friction Angle for Strip Footings

6 Square and Rectangular Footings

Square and rectangular footings with 1:1, 2:1 and 3:1 aspect ratios were investigated, thus having B/L ratios of 0.33, 0.50, and 1.0. Settlement vs. pressure curves for these footings appear essentially the same as the one shown for strip footings (Fig. 2a) except for different values of bearing capacity. The deformed mesh and 3D displacement vectors for a 2 x 4 rectangular footing, soil properties $\phi=20^\circ$ and $c=100$, are shown in Figure 5a and b, respectively, and those for square footings are shown in Figure 6a and b. It may be seen in these figures that even for aspect ratios of only 2:1, the failure mechanism of rectangular footings is dominant on the long side as compared to square footing failures, implying that plane strain behavior starts to dominate quite soon as one side is made longer than the other.

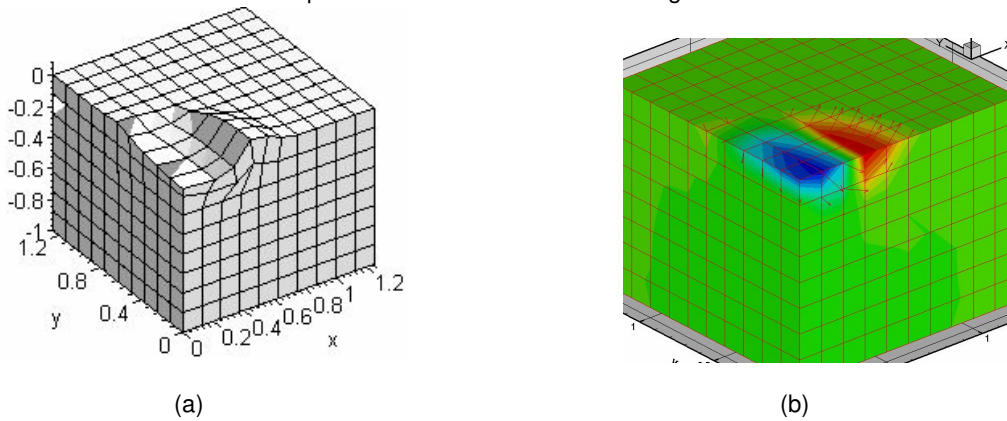


Figure 5. Deformed Mesh and Displacement Vectors for Rectangular Footings

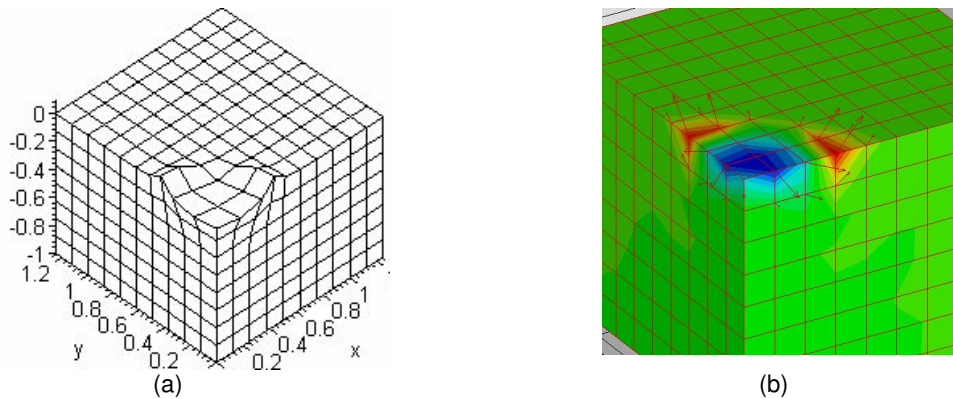


Figure 6. Deformed Mesh and Displacement Vectors for Square Footing

Analyses were performed on square footings to determine how well N_c could be predicted. Cohesion was set to zero and surcharge pressure, q , set to a nominal value of 100 units of pressure. Then, bearing capacity was determined for a range of friction angles. Values determined in this study are shown in Figure 7 along with values determined by equation 8 for $q=0$. It may be seen that there is good agreement between theoretical and finite element-determined values. Similar analyses were performed for a range of footing aspect ratios for the case where q was set to zero, friction angle was 20° , and $c=100$ to compare shape factor values from these analyses to theoretical values. These data may be seen plotted in Figure 8 where it may be seen that the shape factor, s_c , from this study is lower at greater B/L ratios than expected values.

Figure 9 shows results from square footings where the bearing capacity is shown plotted vs. friction angle, for the case where $c=0$ and a surcharge, $q=100$ units of pressure are applied. Since N_q for strip footings was in good agreement between these FEM analyses and the values determined from equation 3, it would appear that the values for shape factor, s_q , account for the differences shown in Figure 7. Shape factor, s_q , is plotted in Figure 10 from the results of this study and from equation 7. It may be seen that the results from this study are much less dependant on friction angle than the results from equation 7. It should be noted that these results are preliminary and certainly do warrant further investigation.

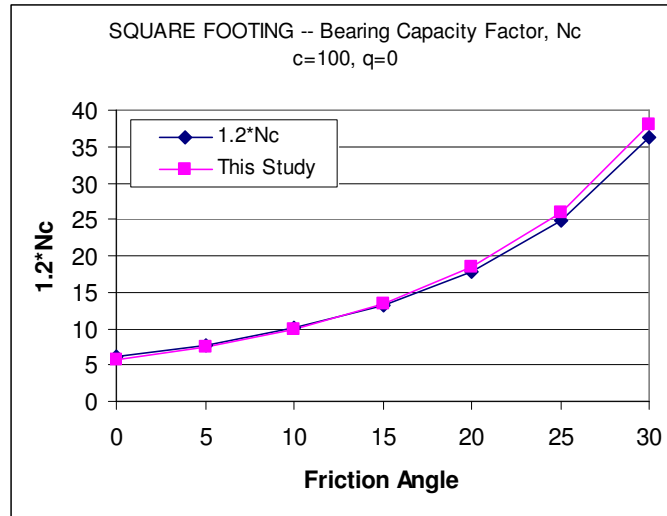


Figure 7. Bearing Capacity ($1.2 \cdot N_c$) vs. Friction Angle for Square Footings

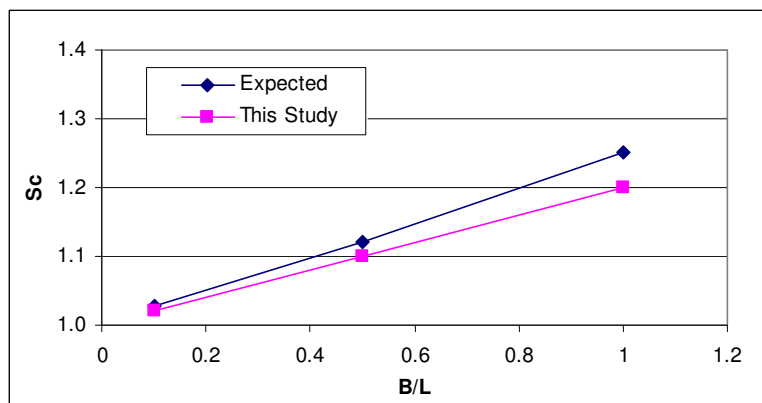


Figure 8. Shape Factor, S_c , vs. B/L Ratios ($\phi=20^\circ$, $c=100$, $q=0$)

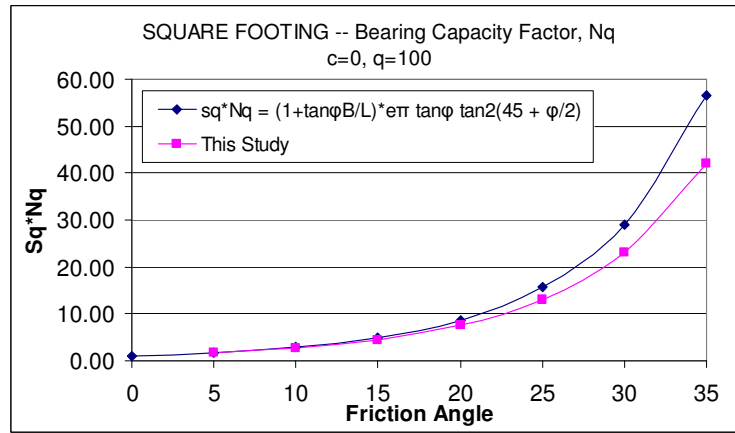


Figure 9. Bearing Capacity ($s_q * N_q$) vs. Friction Angle for Square Footings

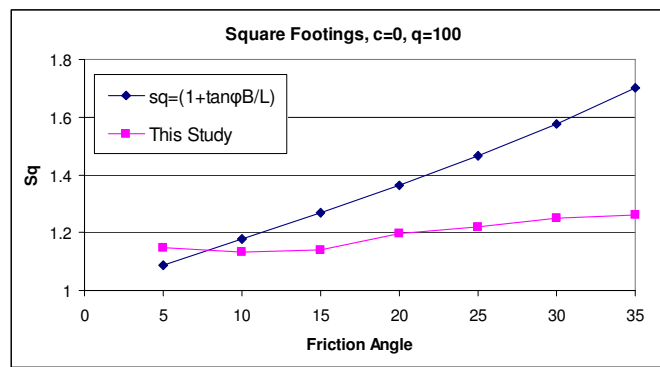


Figure 10. Shape Factor, s_q , vs. Friction Angle for Square Footings

7 Summary And Conclusions

The central point of this paper is to demonstrate that real life 3-D analyses in geomechanics may be accurately performed using finite elements, pcg algorithms, and parallel processing. Bearing capacity factors and failure mechanisms were investigated for weightless, cohesionless soil. Bearing capacity factors N_c and N_q determined in these analyses are very close to theoretical values reported for strip footings. Bearing capacity factor, N_q , for square footings determined in this study were closed to theoretical values for smaller friction angles, but were 15% to 25% lower for larger friction angles. The failure mechanism for rectangular footings is observed to be strongly dominated by the long side of the footing, which should come as no surprise, but that point is clearly illustrated in this paper. The failure mechanism for square footings indicates that much smaller mesh sizes may be used in future analyses without adversely affecting results. Parallel processing is shown to be a valuable tool for performing extensive finite element computations in a reasonable amount of time. If supercomputers are not available, PC Clusters or Beowulfs can provide parallel processing power at a reasonable cost.

This is an on-going project in which a range of soils parameters, including frictional soils, will be investigated.

8 Acknowledgments

The authors gratefully acknowledge the support of the Department of Defense (DOD) High Performance Computing Modernization Program (HPCMP), Dr. Larry P. Davis, Deputy Director, and the resources used at the US Army Research Laboratory (ARL) at Aberdeen Proving Ground, MD.

The support and assistance of LTC Robert Hansen, Mr. Rich Catello, and COL Kip Nygren, USMA, West Point, NY, is gratefully acknowledged.

The support of NATO grant PST.CLG.978469 is gratefully acknowledged.

9 References

- Margetts, L. 2002. "Parallel finite element analysis", PhD thesis, University of Manchester.
- Smith, I.M. 2000. "A general purpose system for finite element analyses in parallel", Eng. Computations 17(1), 75-91.
- Prandtl, L. 1921. On the Penetrating Strengths (Hardness) of Plastic Construction materials and the Strength of Cutting Edges (in German), Zeit. Angew. Math. Mech., 1, No. 1, pp. 15-20.
- Reissner, H. 1924. "Zum Erddruckproblem" (Concerning the earth-pressure problem) Proc. 1st Intl. Congress of Applied Mechanics, Delft, pp. 295-311.
- Skempton, A.W. 1951. The Bearing Capacity of Clays. Proc. British Bldg. Research Congress, 1, pp180-189.
- Smith, I. M. and Griffiths, D. V. 2004. Programming the Finite Element Method, 4th edition, John Wiley publisher, New York, NY.
- Terzaghi, Karl and Peck, Ralph B. 1967. Soil Mechanics in Engineering Practice. Second Edition, John Wiley and Sons. New York, NY, 729p.
- Zienkiewicz, O. C. and Corneau, I. C. 1974. Viscoplasticity, Plasticity and Creep in Elastic Solids, A unified approach. International Journal for Numerical Methods in Engineering, Volume 8, pp. 821-845.